

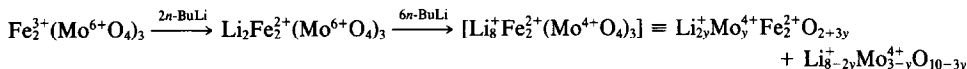
## Lithium Insertion into $\text{Fe}_2(\text{MO}_4)_3$ Frameworks: Comparison of $M = \text{W}$ with $M = \text{Mo}$ \*

A. MANTHIRAM† AND J. B. GOODENOUGH

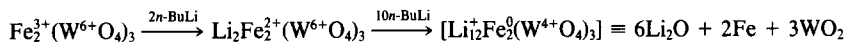
Center for Materials Science and Engineering, ETC II 5.160,  
The University of Texas, Austin, Texas 78712

Received December 8, 1986; in revised form February 23, 1987

Room-temperature lithium insertion into the title framework structures can be represented as



with  $0 < y < 1$  and



Electrochemical insertion/extraction is reversible for  $\text{Li}_x\text{Fe}_2(\text{WO}_4)_3$ ,  $0 \leq x \leq 2.0$ , as in the molybdate system, a two-phase region extending over the range  $0 < x \leq 1.7$ . Lithium insertion suppresses the ferroelastic deformation of the unlithiated framework, but is otherwise topotactic for  $0 \leq x \leq 2.0$ . Chemical delithiation to  $x \approx 0.7$  is possible for the two-phase product  $[\text{Li}_8\text{Fe}_2(\text{MoO}_4)_3]$ . The  $\text{Li}_2\text{Fe}_2(\text{MO}_4)_3$  orthorhombic (*Pbcn*) phases are metastable; they transform to a stable orthorhombic (*Pnma*) structure at 537 K for  $M = \text{Mo}$ , 579 K for  $M = \text{W}$ .  $\text{Li}_2\text{Fe}_2(\text{WO}_4)_3$  disproportionates to  $\text{FeWO}_4$  and  $\text{Li}_2\text{WO}_4$  above 723 K. © 1987 Academic Press, Inc.

### Introduction

Framework structures containing an interconnected interstitial space are potentially fast ionic conductors, particularly if energetically equivalent interstitial sites are connected in three dimensions by a relatively flat intersite potential (*I*). Such structures were first explored for solid electrolytes (2).

If the framework contains a high density

\* Work supported by AFOSR.

† On leave from Madurai Kamaraj University, Madurai, India.

of ions with a redox potential at a convenient energy, reversible topotactic insertion/extraction of a mobile atom is possible. Such insertion/extraction reactions are of technical interest as electrodes for secondary batteries and electrochromic displays; they are also of fundamental interest for low-temperature synthetic routes to new materials.

A number of oxides having the general compositional formula  $A_nM_2(\text{XO}_4)_3$  adopt crystal structures containing a framework of  $\text{XO}_4$  tetrahedra sharing all three corners with  $\text{MO}_6$  octahedra and  $\text{MO}_6$  octahedra sharing all their corners with  $\text{XO}_4$  tetrahe-

dra. The prototype framework is found in the cubic structure of garnet, ideal composition  $\text{Ca}_3\text{Al}_2(\text{SiO}_4)_3$ .

In the garnet structure (3), space group  $Ia\bar{3}d$ , the framework creates eight-coordinated interstitial sites of triangulated dodecahedral symmetry (see Fig. 1); and the three dodecahedral sites per formula unit are completely filled with  $A$  cations.

Distortions of the garnet framework change the character of both the interstitial sites and the intersite potential. For example, langbeinite—with ideal chemical formula  $\text{K}_2\text{Mg}_2(\text{SO}_4)_3$ —contains only two  $A$  cations per formula unit; and in its structure the framework is modified so as to accommodate better the large  $\text{K}^+$  ions. Although the langbeinite structure is also cubic, the symmetry is relaxed to  $P2_13$ , which completely lifts the threefold degeneracy of the interstitial sites. The  $\text{K}^+$  ions occupy a 12-coordinated and a 9-coordinated site; the third interstitial site is greatly reduced in size and remains empty (4).

A distortion of the framework to rhombohedral ( $R\bar{3}c$ ) symmetry creates four octahedral interstitial sites per formula unit that are interconnected in three dimensions by a puckered six-membered ring having its six sides alternately tetrahedral-site and octahedral-site edges of the framework. One of the four interstitial sites per formula unit is inequivalent; it is completely occupied in  $\text{NaZr}_2(\text{PO}_4)_3$  (5). All four sites are occupied in  $\text{Na}_4\text{Zr}_2(\text{SiO}_4)_3$  (6). The mixed system  $\text{Na}_{1+3x}\text{Zr}_2(\text{P}_{1-x}\text{Si}_x\text{O}_4)_3$  contains the  $\text{Na}^+$ -ion electrolyte composition ( $x = \frac{2}{3}$ ) of NAFION, which exhibits a distortion of the framework to monoclinic ( $C2/c$ ) symmetry at room temperature (7). Although this distortion further lifts the degeneracy of the interstitial sites, it does not influence strongly the  $\text{Na}^+$ -ion mobility within the framework.

A number of  $M_2^{3+}(\text{XO}_4)_3^{2-}$  frameworks are stable in the total absence of  $A$  cations; these include molybdates and tungstates of

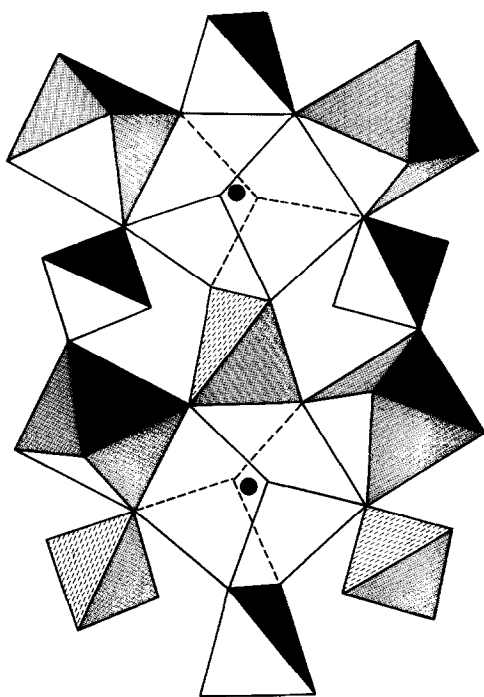


FIG. 1. Linkage of octahedral and tetrahedral sites in the garnet framework; black circles represent dodecahedral site  $A$  cations.

$\text{Al}^{3+}$ ,  $\text{Sc}^{3+}$ ,  $\text{Cr}^{3+}$ ,  $\text{Fe}^{3+}$ ,  $\text{In}^{3+}$ , and the smaller rare-earth ions  $\text{Ln}^{3+}$  as well as ferric sulfate,  $\text{Fe}_2(\text{SO}_4)_3$  (8–19). These compounds crystallize in an orthorhombic ( $Pnca$  or  $Pbcn$ ) symmetry and undergo at lower temperatures a ferroelastic transformation to monoclinic ( $P2_1/a$ ) symmetry. Sleight and Brixner (13) have shown that the transition temperature  $T_t$  increases with increasing electronegativity of the  $M$  cation for any series of molybdates or tungstates. Among the molybdates,  $\text{Fe}_2(\text{MoO}_4)_3$  exhibits the highest transition temperature ( $T_t = 772$  K).

The relationship between the  $\text{Fe}_2(\text{MoO}_4)_3$  and garnet structures was indicated by a cubic growth in the former having a pseudocubic cell parameter  $a_c \approx 12.8$  Å, which is comparable to that observed in many garnets. Plyasova *et al.* (16) determined the

following relationship between the pseudo-cubic unit-cell parameters  $a_c \approx b_c \approx c_c$  and the monoclinic unit-cell parameters:

$$a_c = 2a_m + c_m$$

$$b_c = 2b_m + c_m$$

$$c_c = 2b_m + c_m.$$

The characteristic feature of the  $\text{Fe}_2(\text{MoO}_4)_3$  framework (Fig. 2) is an interstitial space interconnected in three dimensions via puckered six-membered rings having their sides alternately tetrahedral and octahedral edges, as in the NAFION structure. Moreover, the framework contains two reducible cations,  $\text{Fe}^{3+}$  and  $\text{Mo}^{6+}$ , with octahedral  $\text{Fe}^{3+}$  more easily reduced than tetrahedral  $\text{Mo}^{6+}$  (20).

Recently Nadiri *et al.* (21) as well as Reiff *et al.* (22) have shown that lithium can be inserted either electrochemically or chemically into the  $\text{Fe}_2(\text{MoO}_4)_3$  framework to give  $\text{Li}_2\text{Fe}_2(\text{MoO}_4)_3$ . The  $\text{Li}_2\text{Fe}_2(\text{MoO}_4)_3$  structure has the orthorhombic (*Pbcn*) symmetry of high-temperature ( $T > T_i = 772$  K)  $\text{Fe}_2(\text{MoO}_4)_3$ , and the constant open-circuit voltage vs lithium content  $x$  of a  $\text{Li}/\text{Li}_2\text{Fe}_2(\text{MoO}_4)_3$  cell for  $0 \leq x \leq 2.0$  indicates there is little solid solution between the two end-member phases (21). A neutron-diffraction study (23) of  $\text{Li}_2\text{Fe}_2(\text{MoO}_4)_3$  has located the  $\text{Li}^+$  ions in distorted tetrahedral sites formed by the edges of two  $\text{FeO}_6$  octahedra (Fig. 3). This structure represents the first example of a garnet-related framework containing A cations in tetrahedral interstitial sites.

Reiff *et al.* (22) have also used magnetic-susceptibility and Mössbauer measurements to determine a magnetic-ordering temperature of 12.5 K below which a weak ferromagnetism is associated with antiferromagnetically coupled  $\text{Fe}^{2+}$  ions in  $\text{Li}_2\text{Fe}_2(\text{MoO}_4)_3$ . In view of the inequivalence of the two tetrahedral sites of the framework, a Néel type-L antiferromagnetism similar

to that found in  $\text{Fe}_2(\text{SO}_4)_3$  (24) is the more probable origin of the weak ferromagnetism.

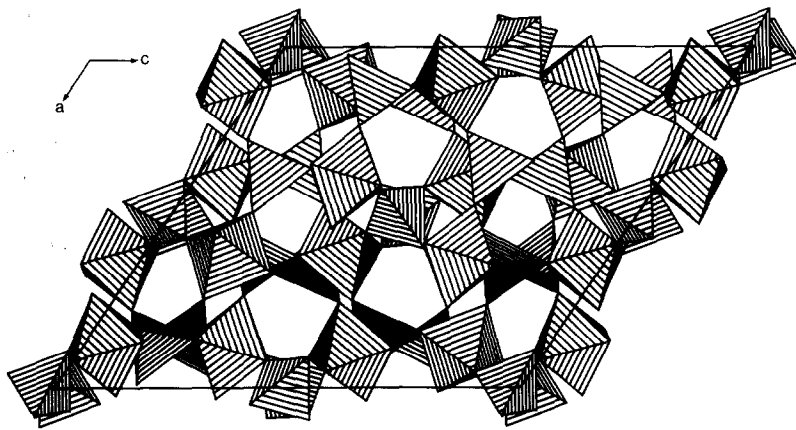
Harrison *et al.* (25) have recently prepared pure  $\text{Fe}_2(\text{WO}_4)_3$  and reported it to be isostructural with room-temperature  $\text{Fe}_2(\text{MoO}_4)_3$ . We have studied both the electrochemical and chemical insertion/extraction reactions of lithium with  $\text{Fe}_2(\text{WO}_4)_3$  prepared by the method of Harrison *et al.*, and we compare below the results obtained with those for the  $\text{Fe}_2(\text{MoO}_4)_3$  framework. Moreover, we extend the lithiation beyond  $x = 2.0$ . In addition, we report on the thermal stabilities of the two  $\text{Li}_2\text{Fe}_2(\text{MO}_4)_3$  compounds,  $M = \text{Mo}$  and  $\text{W}$ , which we have studied with DSC thermal analysis. This technique has also revealed how to prepare a second low-temperature phase of  $\text{Li}_2\text{Fe}_2(\text{WO}_4)_3$ .

## Experimental

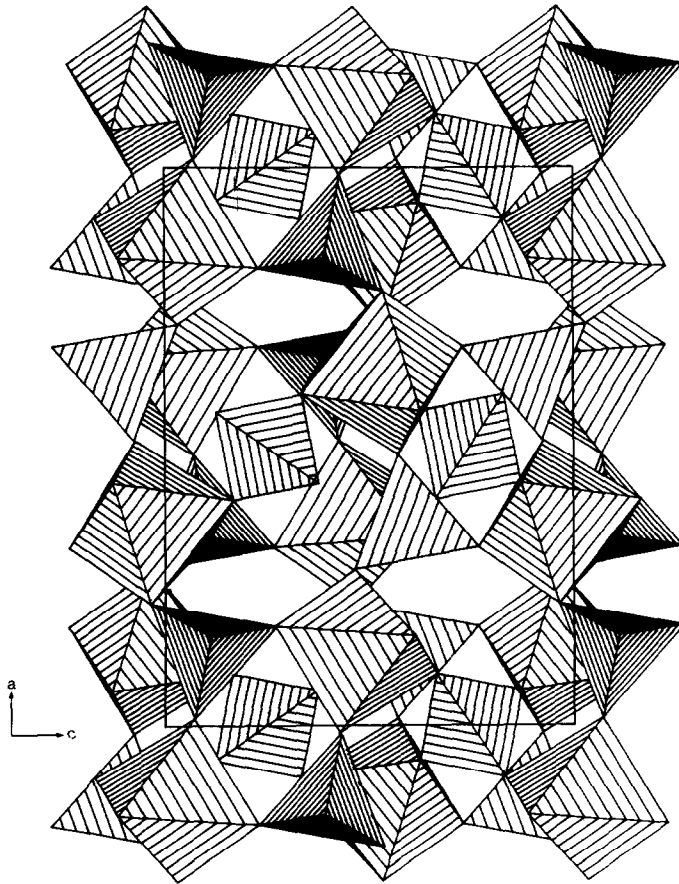
*Synthesis of starting materials.*  $\text{Fe}_2(\text{MoO}_4)_3$  was precipitated from stoichiometric aqueous solutions of ferric nitrate and ammonium molybdate. After boiling for 30 min, the precipitate was filtered, dried at 380 K, and finally heated at 970 K for 15 hr (19).

$\text{Fe}_2(\text{WO}_4)_3$  was prepared by the procedure of Harrison *et al.* (25). A solution of 16.32 g of  $\text{Fe}(\text{NO}_3)_3 \cdot 9\text{H}_2\text{O}$  in 200 ml of water was slowly added under constant stirring with a magnetic stirrer to a solution of 20 g of  $\text{Na}_2\text{WO}_4 \cdot 2\text{H}_2\text{O}$  in 200 ml of water. The creamy yellow precipitate formed was stirred for 30 min, heated to dryness in a steam bath, ground up, washed with distilled water in a Buchner funnel, and dried in a vacuum oven at 373 K for 1 hr. The product was reground, washed with distilled water, dried in a vacuum oven at 373 K for another hour, and finally annealed at 750 K for 8 hr.

The formations of both ferric molybdate

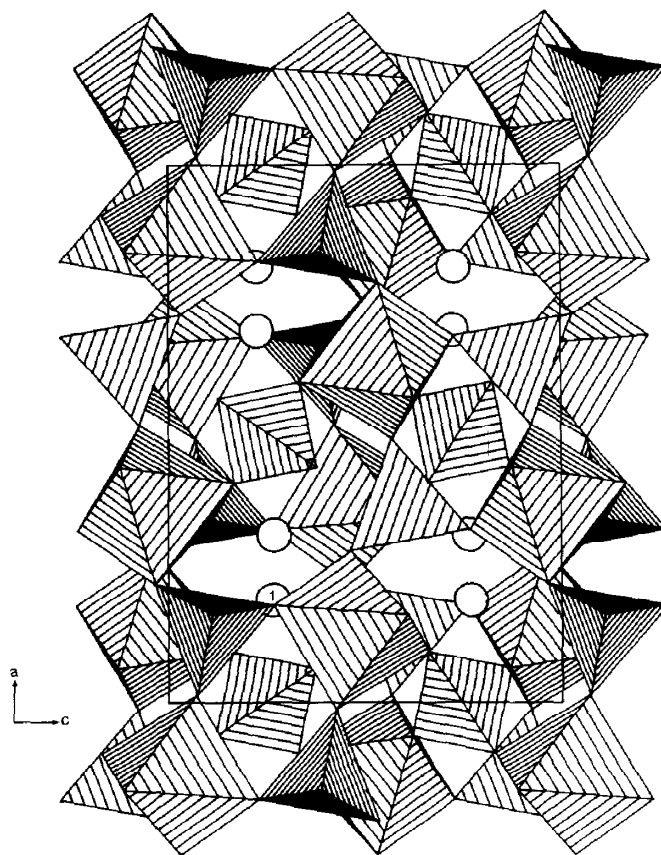


(a)

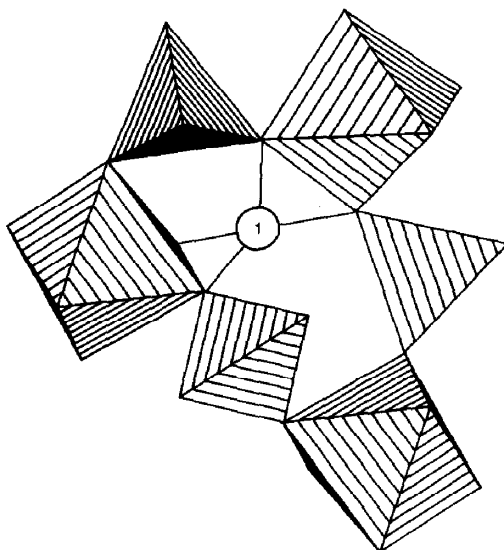


(b)

FIG. 2. Structures of (a) monoclinic ( $P2_1/a$ ) and (b) orthorhombic ( $Pnca$  or  $Pbcn$ )  $\text{Fe}_2(\text{MoO}_4)_3$ .



(a)



(b)

FIG. 3. (a) Structure of orthorhombic (*Pbcn*)  $\alpha\text{-Li}_2\text{Fe}_2(\text{MoO}_4)_3$  and (b) environment of the lithium labeled 1 in (a) showing tetrahedral coordination within a six-membered ring.

and ferric tungstate were confirmed by X-ray diffraction.

**Lithium insertion.** Chemical insertion of lithium into the two frameworks  $\text{Fe}_2(\text{MO}_4)_3$ ,  $M = \text{Mo}$  or  $\text{W}$ , was carried out by reaction with a calculated amount of *n*-butyllithium (Koch light, 15% w/w solution) diluted with dry petroleum spirit (boiling point 40–60°C). The reaction was carried out in a Schlenk flask under dry nitrogen at ambient temperature by continuously stirring with a magnetic stirrer for several days. The product was washed several times with petroleum spirit, dried under vacuum, and transferred into an argon-filled glove box.

Chemical lithiation of  $\text{Fe}_2(\text{WO}_4)_3$  was also carried out by reacting with  $\text{LiI}$  in dry acetonitrile in a Schlenk flask under dry nitrogen, washing the product with acetonitrile, and drying under vacuum.

Electrochemical insertion of lithium into  $\text{Fe}_2(\text{WO}_4)_3$  was studied at a current density of  $15 \mu\text{A cm}^{-2}$  with a cell  $\text{Li}|1 M \text{LiBF}_4$  in propylene carbonate  $|\text{Li}_x\text{Fe}_2(\text{WO}_4)_3$  + graphite. Since ferric tungstate is a poor electronic conductor, 25% (by weight) graphite was mixed with  $\text{Fe}_2(\text{WO}_4)_3$  to improve the

conductivity of the cathode. Cell voltages were allowed to equilibrate for from several hours to a few days in order to obtain a constant reading for the open-circuit voltage.

**Characterization.** The lithium content in the reaction products was estimated by atomic absorption spectroscopy. All the products were analyzed by X-ray powder diffraction. The powder patterns were recorded with a Philips X-ray diffractometer and  $\text{CuK}\alpha$  radiation. DSC analyses were carried out with a heating rate of 10°/min under flowing argon on a Stanton Redcroft 780 instrument.

## Results and Discussion

**Reaction with *n*-butyllithium.** Color changes indicate that both  $\text{Fe}_2(\text{MoO}_4)_3$  and  $\text{Fe}_2(\text{WO}_4)_3$  undergo rapid reaction with *n*-butyllithium.  $\text{Li}_x\text{Fe}_2(\text{MoO}_4)_3$  powders with  $0 < x \leq 2.0$  are dark brown in color; those with  $x > 2.0$  are black.  $\text{Li}_x\text{Fe}_2(\text{WO}_4)_3$  powders with  $0 < x \leq 2.0$  are yellowish gray; those with  $x > 2.0$  are black.

X-ray diffraction (Fig. 4 and Table I) reveals that, for both  $M = \text{Mo}$  and  $M = \text{W}$ ,

TABLE I  
LATTICE PARAMETERS

Compound	Symmetry	<i>a</i> (pm)	<i>b</i> (pm)	<i>c</i> (pm)	$\beta$ (°)	Unit-cell volume $\times 10^{-8}$ (pm <sup>3</sup> )
$\text{Fe}_2(\text{MoO}_4)_3$	Monoclinic ( $P2_1/a$ )	1585	926	1824	125.2	21.88
$\alpha\text{-Li}_2\text{Fe}_2(\text{MoO}_4)_3$	Orthorhombic ( $Pbcn$ )	1291	950	935		11.47
$\beta\text{-Li}_2\text{Fe}_2(\text{MoO}_4)_3$	Orthorhombic ( $Pnma$ )	514	1035	1779		9.46
$\text{Li}_{2y}\text{Mo}_y\text{Fe}_2\text{O}_{2+3y}$ ( $0 < y < 1$ )	Cubic (rocksalt type)	415				
$\text{Fe}_2(\text{WO}_4)_3$	Monoclinic ( $P2_1/a$ )	1595	932	1847	125.7	22.30
$\alpha\text{-Li}_2\text{Fe}_2(\text{WO}_4)_3$	Orthorhombic ( $Pbcn$ )	1295	957	942		11.67
$\beta\text{-Li}_2\text{Fe}_2(\text{WO}_4)_3$	Orthorhombic ( $Pnma$ )	515	1039	1784		9.55

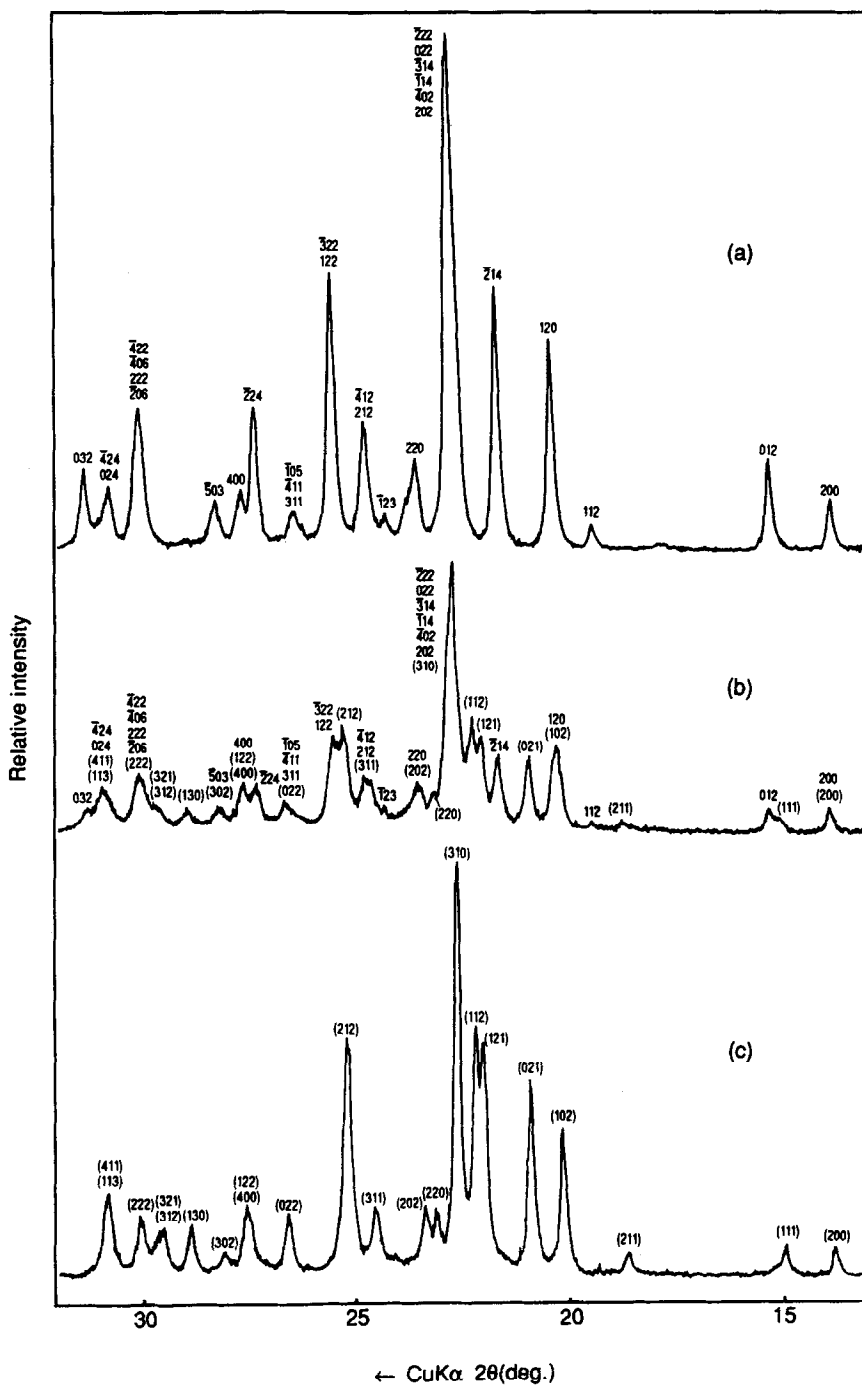
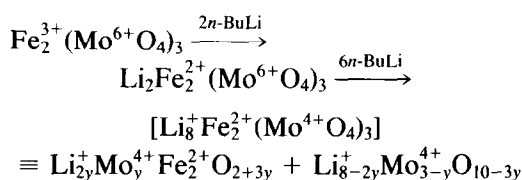


FIG. 4. X-ray diffraction patterns of  $\text{Li}_x\text{Fe}_2(\text{WO}_4)_3$ : (a)  $x = 0$ , (b)  $x = 1.0$ , and (c)  $x = 2.0$ .

the products  $\text{Li}_x\text{Fe}_2(\text{MO}_4)_3$  with  $x = 0.5, 1.0,$  and  $1.5$  are two-phase mixtures of  $\text{Fe}_2(\text{MO}_4)_3$  and  $\text{Li}_{2-y}\text{Fe}_2(\text{MO}_4)_3$ . The powder pattern of the single-phase product  $\text{Li}_2\text{Fe}_2(\text{WO}_4)_3$  could be indexed on an orthorhombic (*Pbcn*) cell similar to that of  $\text{Li}_2\text{Fe}_2(\text{MoO}_4)_3$ . This orthorhombic cell contains an  $\text{Fe}_2(\text{MoO}_4)_3$  framework isostructural with  $\text{Sc}_2(\text{WO}_4)_3$  (10) and the high-temperature ( $T > T_i = 772$  K) form of  $\text{Fe}_2(\text{MoO}_4)_3$  (17, 26). The high-temperature modification of  $\text{Fe}_2(\text{WO}_4)_3$  has not been identified; decomposition to  $\text{Fe}_2\text{WO}_6$  and  $\text{WO}_3$  occurs at higher temperatures ( $T > 800$  K). Nevertheless, the insertion of lithium into monoclinic  $\text{Fe}_2(\text{WO}_4)_3$  suppresses the ferroelastic distortion of the framework just as it does in the molybdate.

Further lithiation of both  $\text{Li}_2\text{Fe}_2(\text{MoO}_4)_3$  and  $\text{Li}_2\text{Fe}_2(\text{WO}_4)_3$  is possible with *n*-butyllithium; this agent can reduce  $\text{Fe}^{2+}$  to  $\text{Fe}^0$  as well as tetrahedral  $\text{Mo}^{6+}$  to octahedral  $\text{Mo}^{4+}$  in an oxide. Lithium analysis shows that  $\text{Fe}_2(\text{MoO}_4)_3$  can take up to 8 lithium atoms per formula unit ( $x = 8$ ) whereas  $\text{Fe}_2(\text{WO}_4)_3$  can take up to 12 lithium atoms per formula unit ( $x = 12$ ). However, in each system the insertion of more than two lithium atoms ( $x > 2.0$ ) is not topotactic; it causes a disproportionation of the framework.

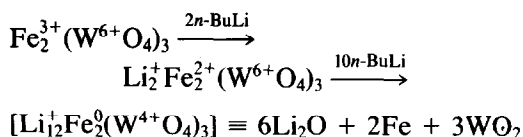
In the molybdate system, X-ray diffraction of the products with  $2.0 < x \leq 8.0$  indicates the presence of a rocksalt-type phase, an amorphous phase with a very broad reflection at  $2\theta \approx 19^\circ$  and—for  $x \neq 8$ —unreacted  $\text{Li}_2\text{Fe}_2(\text{MoO}_4)_3$ . The rocksalt-type phase, which appears only after all the iron has been reduced to the  $\text{Fe}^{2+}$  state, has a lattice constant  $a_0 = 415$  pm, a value distinctly lower than that of  $\text{FeO}$  ( $a_0 = 430.7$  pm (27)). This observation indicates partial substitution of  $\text{Fe}^{2+}$  by the smaller  $\text{Mo}^{4+}$  and  $\text{Li}^+$  ions,  $3\text{Fe}^{2+} = 2\text{Li}^+ + \text{Mo}^{4+}$ . We can therefore represent the reaction of  $\text{Fe}_2(\text{MoO}_4)_3$  with *n*-butyllithium as follows,



with  $0 < y < 1$ . It is known (28, 29) that reaction of  $\text{Li}_2\text{O}$  or  $\text{LiOH}$  with  $\text{MoO}_2$  below 970 K yields cubic phases in the compositional range  $\text{Li}_2\text{MoO}_3\text{--Li}_6\text{Mo}_2\text{O}_7$ , and we have assumed that a solid solution of  $\text{Fe}_{1-\delta}\text{O}$  and  $\text{Li}_2\text{MoO}_3$  is not only possible, but contains no  $\text{Fe}^{3+}$ . Delithiation with bromine (see below) is consistent with this assumption. The broad X-ray diffraction peak at  $2\theta \approx 19^\circ$  for the "amorphous" phase corresponds to a strong reflection in the low-temperature form of the system  $\text{Li}_2\text{MoO}_3\text{--Li}_6\text{Mo}_2\text{O}_7$ ; moreover, this peak became somewhat sharper after the product was heated in argon for 1 hr at about 800 K. Unfortunately, the other expected reflections for the lithium-molybdenum oxide overlap with those of the rocksalt-type phase, so it was not possible to make an unambiguous identification of the amorphous phase in this system.

In contrast, insertion of more than two lithium into  $\text{Fe}_2(\text{WO}_4)_3$  gives predominantly amorphous phases only. Although traces of a rocksalt-type phase were found for  $x > 2.0$ , this product appears to be unstable, unlike the corresponding phase in the molybdate system. We therefore conclude that  $\text{W}^{4+}$  differs from  $\text{Mo}^{4+}$  by being unable to stabilize with  $\text{Li}^+$  the rocksalt-type phase. This conclusion is consistent with the observation (29) that a large number of ternary oxides containing  $\text{Mo}^{4+}$  are known, but those with  $\text{W}^{4+}$  are very rare. In view of the instability of the intermediate rocksalt-type phase and the uptake of 12 lithium per formula unit in the tungstate system, we represent the reaction of ferric tungstate with *n*-butyllithium as follows:





This formulation is consistent with the observation (30, 31) that lithiation of  $\text{Fe}_3\text{O}_4$  and  $\text{Fe}_2\text{O}_3$  in excess of that required to reduce all  $\text{Fe}^{3+}$  to  $\text{Fe}^{2+}$  displaces some of the iron from the oxide lattice as elemental Fe. At  $420^\circ\text{C}$ , extruded  $\text{Fe}^0$  forms particles of sufficient size to give an identifiable powder X-ray-diffraction pattern (30); at room temperature the iron extruded from  $\text{Li}_{2+x}\text{Fe}_2(\text{WO}_4)_3$  would appear to remain in clusters too small for X-ray identification.

The fact that no more than two lithium per formula unit are introduced topotactically into the  $\text{Fe}_2(\text{MO}_4)_3$ ,  $M = \text{Mo}$  or  $\text{W}$ , framework can be rationalized as follows: (i) In  $\text{Li}_2\text{Fe}_2(\text{MoO}_4)_3$ —and presumably also in  $\text{Li}_2\text{Fe}_2(\text{WO}_4)_3$ —the crystallographically equivalent tetrahedral sites occupied by  $\text{Li}^+$  ions are completely filled (Fig. 3). Further lithiation into the interstitial space of the framework would require overcoming the additional electrostatic energy associated with occupancy of another subarray of sites. (ii) The  $\text{Mo}^{6+}$  and  $\text{W}^{6+}$  ions are in tetrahedral sites that are isolated from one another, which raises their associated empty  $d$  levels at least 1 eV above a  $d$  state associated with  $\text{Mo-Mo}$  or  $\text{W-W}$  bonding across a shared octahedral-site edge. Therefore the reduced ions have a definite octahedral-site preference even where formation of a  $(\text{Mo} = \text{O})^{3+}$  ion induces a shift of the cation from the center of symmetry of the site.

*Reaction with LiI:* Lithium iodide is a significantly milder reducing agent than  $n$ -butyllithium, but it is capable of reducing  $\text{Fe}^{3+}$  to  $\text{Fe}^{2+}$  in both systems; it does not reduce  $\text{Mo}^{6+}$  or  $\text{W}^{6+}$ . Therefore reaction with  $\text{LiI}$  can yield  $\text{Li}_2\text{Fe}_2(\text{MO}_4)_3$ ,  $M = \text{Mo}$  or  $\text{W}$ , but it cannot cause disproportion-

ation of the framework. Although ferric molybdate has been reported (22) to give  $\text{Li}_2\text{Fe}_2(\text{MoO}_4)_3$  with only a fourfold excess of  $\text{LiI}$ , such a reaction with ferric tungstate results in a mixture of  $\text{Li}_2\text{Fe}_2(\text{WO}_4)_3$  and  $\text{Fe}_2(\text{WO}_4)_3$ . However, reaction of 600 mg of  $\text{Fe}_2(\text{WO}_4)_3$  with a 10-fold excess of  $\text{LiI}$  in 25 ml of dry acetonitrile for 2 weeks gave a single  $\text{Li}_2\text{Fe}_2(\text{WO}_4)_3$  phase. Thus  $\text{Fe}_2(\text{WO}_4)_3$  reacts with  $\text{LiI}$  similarly to  $\text{Fe}_2(\text{MoO}_4)_3$ , but the iron appears to be somewhat more difficult to reduce in the tungstate.

*Reversibility.* Lithium can be extracted from  $\text{Li}_2\text{Fe}_2(\text{MO}_4)_3$ ,  $M = \text{Mo}$  or  $\text{W}$ . Reaction with 0.1  $N$  bromine in dry acetonitrile under dry nitrogen yields the original monoclinic framework phase  $\text{Fe}_2(\text{MO}_4)_3$  with essentially no change in lattice parameter. Thus the ferroelastic transition is seen to be reversible with lithium insertion/extraction as well as with raising and lowering the temperature through  $T_1$ . Therefore we are justified in referring to the lithium insertion/extraction reaction as topotactic even though it is accompanied by a ferroelastic symmetry change of the framework.

On the other hand, the products of the bromine reaction were not completely free of lithium; from 0.1 to 0.2 lithium per formula unit were detected by atomic absorption spectroscopy. In view of the similarity of the lattice parameters of the initial and delithiated frameworks, there is no evidence that lithium has any significant solubility in the monoclinic framework, so we conclude that the lithium resides in unreacted particles. The ease of delithiation appears to depend on particle size and/or surface layers in many insertion/extraction reactions (31).

There is no evidence for a  $\text{Li}_2\text{Fe}_2(\text{MO}_4)_3$  phase remaining at the center of a particle, so it appears that, although extraction occurs at the surface, the  $\text{Fe}_2(\text{MO}_4)_3$  phase is nucleated near the center of a particle and grows out to the surface. Such a growth

implies good lithium mobility in at least one of the two phases and hence some solid solubility. From the open-circuit-voltage curve (see below) any solid solubility in the monoclinic phase is very limited. Therefore we expect some range of solid solution,  $\text{Li}_{2-y}\text{Fe}_2(\text{MoO}_4)_3$ , in the orthorhombic phase.

**Reaction with bromine.** Reaction of the extensively lithiated sample  $\text{Li}_8\text{Fe}_2(\text{MoO}_4)_3$  with 0.1 *N* bromine in acetonitrile reduces the lithium content of the oxide to about 0.7 lithium per  $\text{Fe}_2(\text{MoO}_4)_3$ . The X-ray-diffraction pattern of the delithiated product shows that the rocksalt-type and amorphous phases are still intact. These results show that bromine extracts topotactically a major portion of the lithium from both phases, which is consistent with the observation (32) that  $\text{Li}_2\text{MoO}_3$  can be delithiated topotactically with bromine in acetonitrile to yield  $\text{Li}_x\text{MoO}_3$  ( $x \approx 0.3$ ).

**Open-circuit voltage.** The open-circuit voltage  $V_{oc}$  versus lithium content  $x$  for a  $\text{Li}/\text{Li}_x\text{Fe}_2(\text{WO}_4)_3$  cell (Fig. 5) shows a plateau in the region  $0 < x < 1.7$ , which substantiates the two-phase character of this compositional range with little, if any, solubility of lithium in the monoclinic framework. Moreover, if the presence of graphite in the electrode is not introducing a spurious effect, the curve indicates a solid solution in the orthorhombic phase over the compositional range  $1.7 < x \leq 2.0$ , or  $\text{Li}_{2-y}\text{Fe}_2(\text{WO}_4)_3$  with  $0 \leq y < 0.3$ . This finding thus supports the deductions made from the chemical-delithiation study. The sharp drop in  $V_{oc}$  at  $x = 2.0$  is due to lattice disproportionation and the reduction of  $\text{W}^{6+}$ .

From the equilibration times, it is evident that the lithium-ion diffusion rate is initially fast; it decreases somewhat with increasing  $x$ , but becomes much slower for  $x > 1.5$ . At the higher lithium concentrations, the initial polarization was greater, and several days were required to establish equilibrium. This observation indicates that there are regions

in the electrode where the mobility of the two-phase interface is low. At lower values of  $x$ , the more mobile interfaces move into a particle first, but their area diminishes with increasing  $x$ . Beyond  $x = 1.5$ , many of these interfaces have completely disappeared with the total conversion of individual particles to the new phase.

Recharging at  $15 \mu\text{A cm}^{-2}$  between open-circuit equilibrations demonstrated excellent reversibility over the entire compositional range  $0 < x < 2.0$  (see Fig. 5). For  $x > 0.6$ , recharging was smooth with little polarization, and the cell voltage equilibrated in a few hours. For  $x < 0.6$ , the cell voltage increased by about 300 mV when current was passing—whereas in the  $\text{Li}_x\text{Fe}_2(\text{MoO}_4)_3$  system it increased by 1 V (21)—and the voltage equilibrated in 1 or 2 days. Since recharging, like discharging, involves the nucleation and growth of a second phase, the reciprocity of the discharge/charge cycle supports the interpretation that slower equilibration at the end of a half-cycle reflects a smaller interface area and the disappearance of the more mobile interfaces.

**Thermal analysis.** DSC curves for both  $\text{Li}_2\text{Fe}_2(\text{MoO}_4)_3$  and  $\text{Li}_2\text{Fe}_2(\text{WO}_4)_3$  are given in Fig. 6. The irreversible exotherm in the molybdate curve at 537 K represents transformation of the metastable phase—designated  $\alpha\text{-Li}_2\text{Fe}_2(\text{MoO}_4)_3$ —to the stable

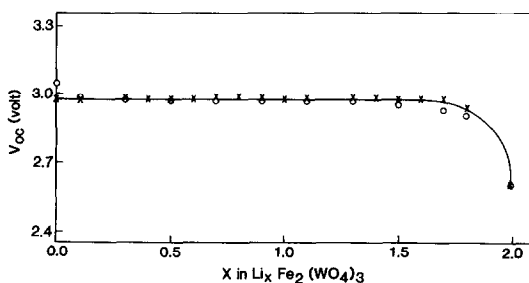


FIG. 5. Open-circuit voltage vs lithium content in  $\text{Li}_x\text{Fe}_2(\text{WO}_4)_3$ ;  $\circ$  and  $\times$  refer to lithiation and delithiation, respectively.

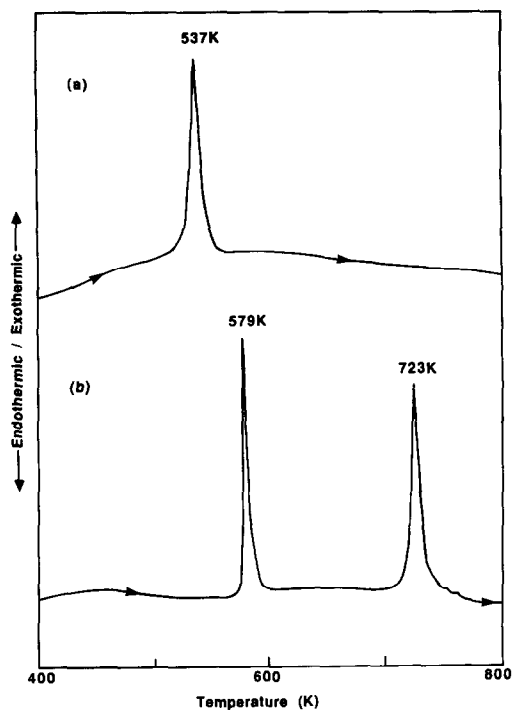


FIG. 6. DSC curves of (a)  $\text{Li}_2\text{Fe}_2(\text{MoO}_4)_3$  and (b)  $\text{Li}_2\text{Fe}_2(\text{WO}_4)_3$ .

$\beta$  form having the orthorhombic ( $Pnma$ ) structure illustrated in Fig. 7. The orthorhombic ( $Pbcn$ )  $\alpha$ -phase is only accessible via a low-temperature synthetic route. The unit-cell parameters (Table I) for the  $\beta$ - $\text{Li}_2\text{Fe}_2(\text{MoO}_4)_3$  obtained by heating  $\alpha$ - $\text{Li}_2\text{Fe}_2(\text{MoO}_4)_3$  above 570 K agree closely with those reported (33, 34) for  $\text{Li}_2\text{Fe}_2(\text{MoO}_4)_3$  obtained by high-temperature ceramic methods.

The DSC curve for  $\text{Li}_2\text{Fe}_2(\text{WO}_4)_3$ , on the other hand, shows two irreversible exotherms at 579 and 723 K. X-ray examination of the products revealed that the exotherm at 579 K is analogous to that in the molybdate system at 537 K; it signals a transformation from the metastable orthorhombic ( $Pbcn$ )  $\alpha$  modification to the stable orthorhombic ( $Pnma$ )  $\beta$  form. The second irreversible exotherm at 723 K is due to a disproportionation of the  $\beta$  modification to  $\text{FeWO}_4$  and  $\text{Li}_2\text{WO}_4$ . The disproportionation above 723 K accounts for the failure of previous workers to obtain a  $\text{Li}_2\text{Fe}_2(\text{WO}_4)_3$  phase by high-temperature tech-

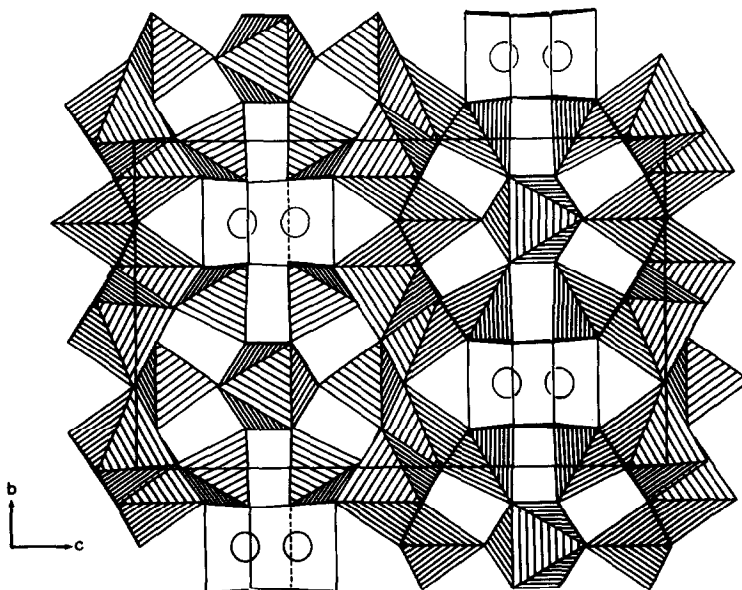


FIG. 7. Structure of orthorhombic ( $Pnma$ )  $\beta$ - $\text{Li}_2\text{Fe}_2(\text{MO}_4)_3$ ,  $M = \text{Mo}$  or  $\text{W}$ .

niques. This example demonstrates the utility of "soft" chemistry as a synthetic route to stable as well as metastable phases.

*Unit-cell volumes.* Table I gives the unit-cell volumes as well as the lattice parameters of the several phases encountered in this study. The orthorhombic  $\text{Li}_2\text{Fe}_2(\text{MoO}_4)_3$  phases contain four formula units per unit cell ( $Z = 4$ ), whereas the monoclinic  $\text{Fe}_2(\text{MoO}_4)_3$  phases have eight ( $Z = 8$ ). Comparison of the volumes of the  $\alpha$ - $\text{Li}_2\text{Fe}_2(\text{MoO}_4)_3$  phases with the half-volumes of the  $\text{Fe}_2(\text{MoO}_4)_3$  phases shows that lithium insertion has increased the volume; the increase reflects primarily the increase in size of the iron ion on going from  $\text{Fe}^{3+}$  to  $\text{Fe}^{2+}$ .

More interesting, perhaps, is the 18% decrease in cell volume on going from the  $\alpha$  to the  $\beta$  modification. The  $\alpha$  form contains an open framework of corner-shared tetrahedra and octahedra; the  $\beta$  form, on the other hand, contains  $\text{Fe}^{2+}$  ions in both face-sharing and edge-sharing octahedra as well as  $\text{Li}^+$  ions in trigonal prisms (33) rather than tetrahedral sites, Fig. 7. The high  $\text{Li}^+$ -ion mobility is seen to be associated with the metastable, open framework of the  $\alpha$  modification.

## References

1. J. B. GOODENOUGH, "Solid Electrolytes" (P. Hagemuller and W. Van Gool, Eds.), Chap. 23, p. 393, Academic Press, New York (1978).
2. J. B. GOODENOUGH, H. Y-P. HONG, AND J. A. KAFALAS, *Mater. Res. Bull.* **11**, 203 (1976).
3. W. PRANDL, *Z. Kristallogr.* **123**, 81 (1966).
4. A. ZEMANN AND J. ZEMANN, *Acta Crystallogr.* **10**, 409 (1957).
5. L-O. HAGMAN AND P. KIERKEGAARD, *Acta Chem. Scand.* **22**, 1822 (1968).
6. R. G. SIZOVA, A. A. VORONKOV, N. G. SHUMYATSKAYA, V. V. PYAKHIM, AND N. V. BELOV, *Dokl. Akad. Nauk SSSR. Ser.* **205**, 90 (1972).
7. H. Y-P. HONG, *Mater. Res. Bull.* **11**, 173 (1976).
8. P. A. KOKKOROS, *Minér. Petrog. Mitt.* **10**, 45 (1965).
9. K. NASSAU, H. J. LEVINSTEIN, AND G. M. LOIACONA, *J. Phys. Chem. Solids* **26**, 1805 (1965).
10. S. C. ABRAHAMS AND J. L. BERNSTEIN, *J. Chem. Phys.* **45**, 2745 (1966).
11. E. YA. RODE, G. V. LYSANOVA, V. G. KUZNETSOV, AND L. Z. GOKHMAN, *Russ. J. Inorg. Chem.* **13**, 678 (1968).
12. D. C. CRAIG AND N. C. STEPHENSON, *Acta Crystallogr. B* **24**, 1250 (1968).
13. A. W. SLEIGHT AND L. H. BRIXNER, *J. Solid State Chem.* **7**, 172 (1973).
14. L. H. BRIXNER, *Rév. Chim. Minér.* **10**, 47 (1973).
15. L. M. PLYASOVA, R. F. KLEVTSOVA, S. V. BORISOV, AND L. M. KEFELI, *Sov. Phys. Dokl.* **11**, 189 (1966).
16. L. M. PLYASOVA, S. V. BORISOV, AND N. V. BELOV, *Sov. Phys. Crystallogr.* **12**, 25 (1967).
17. L. M. PLYASOVA, *J. Struct. Chem.* **17**, 637 (1976).
18. H.-Y. CHEN, *Mater. Res. Bull.* **14**, 1583 (1979).
19. M. H. RAPPOSH, J. B. ANDERSON, AND E. KOSTINER, *Inorg. Chem.* **19**, 3531 (1980).
20. J. B. GOODENOUGH, "Proceedings of the Climax Fourth International Conference on the Chemistry and Uses of Molybdenum" (H. F. Barry and P. C. H. Mitchell, Eds.), p. 1, Climax Molybdenum Co., Ann Arbor, MI (1982).
21. A. NADIRI, C. DELMAS, R. SALMON, AND P. HAGENMULLER, *Rév. Chim. Minér.* **21**, 537 (1984).
22. W. M. REIFF, J. H. ZHANG, AND C. C. TORARDI, *J. Solid State Chem.* **62**, 231 (1986).
23. C. C. TORARDI AND E. PRINCE, *Mater. Res. Bull.* **21**, 719 (1986).
24. G. J. LONG, G. LONGWORTH, P. BATTLE, A. K. CHEETHAM, R. V. THUNDATHIL, AND D. BEVERIDGE, *Inorg. Chem.* **18**, 264 (1979).
25. W. T. A. HARRISON, U. CHOWDHRY, C. J. MACHIELS, A. W. SLEIGHT, AND A. K. CHEETHAM, *J. Solid State Chem.* **60**, 101 (1985).
26. V. MASSAROTTI, G. FLOR, AND A. MARINI, *J. Appl. Crystallogr.* **14**, 64 (1981).
27. B. T. M. WILLIS AND H. P. ROOKSBY, *Acta Crystallogr.* **6**, 827 (1953).
28. J.-M. RÉAU, C. FOUASSIER, AND C. GLEITZER, *Bull. Soc. Chim. France*, 4294 (1967).
29. A. MANTHIRAM AND J. GOPALAKRISHNAN, *Rev. Inorg. Chem.* **6**, 1 (1984).
30. M. M. THACKERAY, W. I. F. DAVID, AND J. B. GOODENOUGH, *Mater. Res. Bull.* **17**, 785 (1982); *J. Solid State Chem.* **55**, 280 (1984).
31. J. FONTCUBERTA, J. RODRIGUEZ, M. PERNET, G. LONGWORTH, AND J. B. GOODENOUGH, *J. Appl. Phys.* **59**, 1918 (1986).
32. A. C. JAMES AND J. B. GOODENOUGH, to be published.
33. R. F. KLEVTSOVA AND S. A. MAGARILL, *Sov. Phys. Crystallogr.* **15**, 611 (1971).
34. P. V. KLEVTSOV, *Sov. Phys. Crystallogr.* **15**, 682 (1971).